文章编号:1000-0550(2016)06-1044-13 doi:10.14027/j.cnki.cjxb.2016.06.004

重晶石沉积类型及成因评述
——兼论扬子地区下寒武统重晶石的富集机制

周锡强[1] 遇 昊[2] 黄泰誉[1,3] 张力钰[1,3] 张恭境[1,3] 付 勇[4] 陈代钊[1]

(1.中国科学院地质与地球物理研究所油气资源研究室 北京 100029;2.中国五矿集团公司 北京 100007;
3.中国科学院大学 北京 100049;4.贵州大学资源与环境工程学院 贵阳 550025)

摘 要 重晶石沉积类型丰富,具有多种成因过程。通常,沉积型重晶石可分为生物、热液、成岩和冷泉重晶石四种类型。富钡与富硫酸盐的流体(海水、早成岩孔隙水或热液流体)及其相互作用过程(水柱、热液系统、沉积柱、沉积物—水界面附近)决定了重晶石的沉积环境、宏微观产出方式、同位素组成及相应的地质意义。另外,根据扬子地区下寒武统富重晶石沉积的地质特征,简述了其各种富集机制的适用性及争论。据此建议,结合埃迪卡拉纪—寒武纪转折时期的古海洋背景,对其进行详细的沉积学及地球化学分析,有助于深化成因认识,弥合分歧。

关键词 重晶石 古海洋 下寒武统

第一作者简介 周锡强 男 1985年出生 博士 沉积学 E-mail:zhouxiqiang123@163.com

中图分类号 P619.25^{+}1 **文献标识码** A

0 引言

重晶石($BaSO_4$)是沉积岩(物)里的常见矿物,自太古宙至今时有发育,并具有层状、条带状、结核状、以及弥散状等多种产出形式[1-4]。重晶石具有高密度(~4.5 g/cm^3)的物理特性,在化工添加剂、油气勘探钻井液等方面具有广泛的工业应用。因此,重晶石的显著富集,具有重要的经济价值。

另一方面,在地质历史时期,重晶石产出丰度具有非均匀的时空分布特征[1,5-6],并可能响应了海洋环境的变化[7]。在矿物成分方面,重晶石富含S、O元素,其相关同位素($\delta^{34}S$、$\delta^{18}O$及$\delta^{17}O$)可用于解译硫循环或古气候特征[3,8-12]。同时,重晶石具有高Sr、低Rb含量特征,是获取$^{87}Sr/^{86}Sr$同位素比值的重要矿物[2]。由于分布广、易保存,重晶石的同位素特征已广泛应用于流体演化[13-16]、全球海水Sr、S同位素组分重建等方面的研究[17-19]。此外,重晶石可以作为古生产力指标[20-22]、硫酸盐—甲烷转换带沉积指示物[23-24]或冷泉流体的活动的记录者等[25-27],具有广泛的地质应用。然而,沉积型重晶石可能源于多种形成过程,并具有不同的成因类型和地质意义。因此对沉积型重晶石的地质特征和成因类型进行对比认识,有助于合理解读其在古海洋、古环境及古地理方面的意义。

本文拟从钡的海洋地球化学循环,并根据重晶石的沉积过程、形成环境、宏微观特征(产出形式、晶体形态)、同位素组成(Sr和S)、以及地质意义等方面对沉积型重晶石进行分类和评述。在此基础上,针对扬子地区下寒武统黑色岩系重晶石富集程度差异、地质特征,对其富集机理进行对比、评述,并指出下一步研究中需注意的问题。

1 海洋钡的循环与分布

现今海洋钡的滞留时间较短,约为8 000年[28]。海洋水柱和沉积物里,钡可赋存于多种物相,包括碳酸盐岩、有机质、硅质、铁锰氧化物、陆源碎屑和海相铝硅酸盐矿物,以及重晶石等[29];其中重晶石矿物是固相钡的主要赋存态[30]。通常,重晶石过饱和沉淀主要源于富Ba^{2+}与富SO_4^{2-}流体的相互作用:$Ba^{2+}+SO_4^{2-}\rightleftharpoons BaSO_4$。由于$BaSO_4$通常具有极低的溶度积(常温常压下约为$1\times10^{-10}$)[31],因此自然界流体只能独立维持高含量的溶解钡或者硫酸盐。现今海水富含SO_4^{2-}(平均浓度为28 mM),但亏损Ba^{2+}(平均浓度约为65 nM)。虽然同时存在一定量的硫酸盐和溶

收稿日期:2016-05-19;**收修改稿日期**:2016-07-04
基金项目:国家自然科学基金面上项目(41472089,41502117);中国博士后科学基金资助项目(2015M581166)[**Foundation**:National Narural Science Foundation of China,No. 41472089, 41502117;China Postdoctoral Science Foundation Funded Project,No. 2015M581166]

解钡,但热力学计算显示现今海洋总体处于重晶石不饱和状态[32-34],因此制约着它的形成和分布。通常,重晶石微颗粒形成于水柱上部[35-36],但随后在水柱中下部及沉积物里经历部分溶解[37-38]。因此,海洋水柱同时存在 Ba 的源和汇,溶解 Ba 含量总体呈现随深度逐渐增加的趋势。现今开阔海洋钡离子浓度约为 20 nM,向深部逐渐增加至约 150 nM[39]。在缺氧盆地,水柱里钡离子浓度(如黑海 50 米以下水柱)可达 500 nM 以上[40]。此外,地下水和河水具有较高的溶解钡含量,受其影响的滨岸和河口等水域相对更为富集溶解钡[41-42]。另一方面,海底热液流体也不同程度的富集钡离子(浓度可达 80 μM 以上)[43],是海洋钡的重要来源之一[44]。

2　重晶石沉积分类

海洋里的重晶石可形成于多种地质过程,并最终保存于沉积物里(或富集为沉积型矿床);在此概称为沉积型重晶石。沉积型重晶石有多种分类方案[2]。根据构造背景和产出特征,Maynard *et al.*[45] 和 Maynard *et al.*[46]将沉积型层状重晶石矿床分为两大类:①大陆边缘类型,纯重晶石矿床,不伴生 Pb、Zn 矿床;②克拉通裂谷型,可能伴生 Pb、Zn 矿床。根据产出形式、流体来源和现今实例,层状重晶石可也分为成岩交代、热液喷流和生物成因类型[1,47]。根据富钡流体来源及与硫酸盐相互作用过程,最新研究成果将海洋重晶石分为四类:生物重晶石、热液重晶石、成岩重晶石和冷泉重晶石(图 1)[48-50]。各类型重晶石在地层沉积记录里广泛报道。由于形成环境和过程差异,如水柱、热液系统、沉积物—水界面附近、或者沉积物柱孔隙环境等,重晶石具有多种晶体习性和结构、产出形式,以及 Sr、S 同位素特征(表 1)[48-49,51]。为了便于科研实践,本文将据此对海洋重晶石沉积类型进行详细介绍。

2.1　生物重晶石

生物重晶石是指在生物直接诱导(胞内合成)或间接调控(有机质降解微环境)作用下形成的重晶石[20,35-36,54](图 1A)。重晶石微晶颗粒形成于不饱和海水,普遍认为与生物有关。研究发现,为维持定向

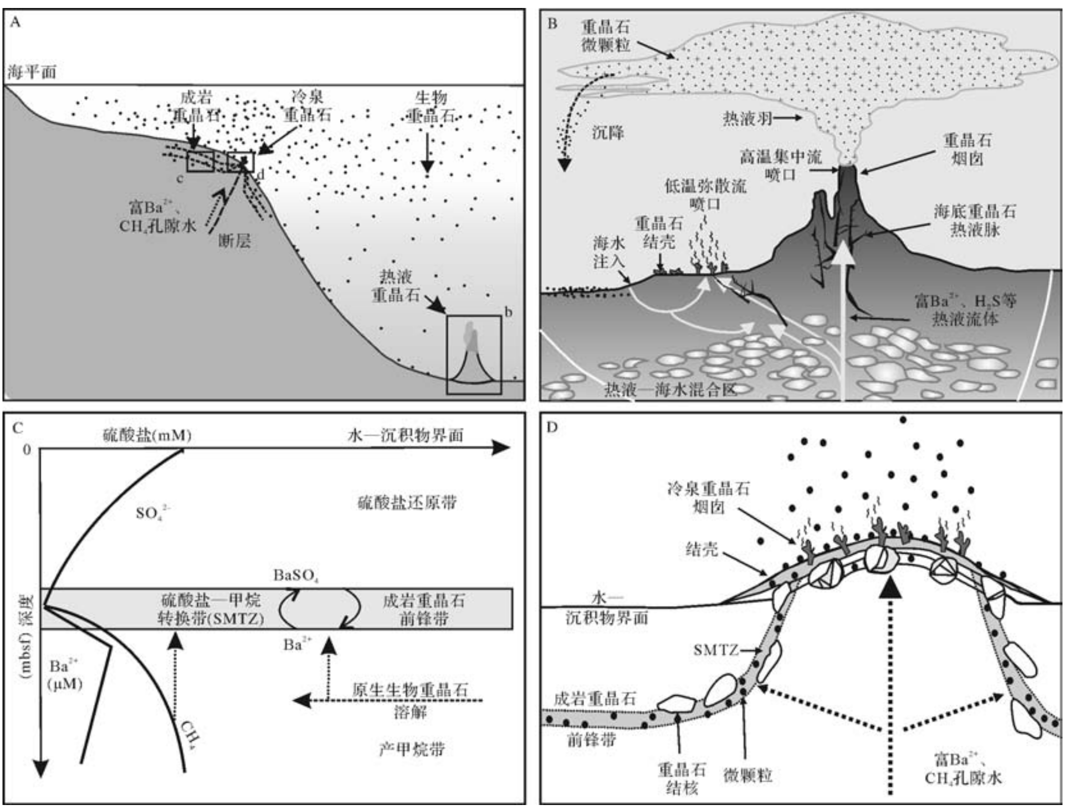

图 1　A. 海洋沉积型重晶石的产出环境;B. 热液重晶石形成模式(修改自文献[52]),图 A 中 b 框细节图;C. 成岩重晶石形成模式,图 A 中 c 框细节图;D. 冷泉重晶石形成模式(修改自文献[53]),图 A 中 d 框细节图。注意成岩重晶石与冷泉重晶石的成因联系。

Fig.1　A. The occurrences of sedimentary barites in marine environments. B. Formation of hydrothermal barite (details of inset box b in Fig. 1A), modified from reference[52]. C. Formation of diagenetic barite (details of inset box c in Fig. 1A). D. Formation of cold seeps barite (details of inset box d in Fig. 1A), modified from reference[53]. Note the genetic connection between the diagenetic and cold seeps barites

表1 沉积型重晶石成因分类和地质特征

Table 1 Genetic classification and geological features of sedimentary barites

重晶石成因类型	生物重晶石	热液重晶石	成岩重晶石	冷泉重晶石
沉积过程	生物直接胞内合成，或有机质降解微环境里生成	富 Ba^{2+} 热流体与含 SO_4^{2-} 流体混合	富 Ba^{2+}(或和 CH_4)孔隙水与含 SO_4^{2-} 孔隙水混合	富 Ba^{2+}(或和 CH4)孔隙水与含 SO_4^{2-} 海水(或孔隙水)混合
钡源	海水及含钡有机质	淋滤洋壳、陆壳及富钡沉积物	早期沉积物(原生生物重晶石等)	早期沉积物(原生生物重晶石等)
硫酸盐源	海水	海水或热液 H_2S 氧化产物	孔隙水(经 BSR 改造后的残余海水硫酸盐)	经 BSR 改造后的孔隙水或海水
形成地点	水柱	热液系统(通道、喷口、热液羽)	沉积物—水界面之下沉积物孔隙环境	沉积物—水界面附近孔隙环境及水柱
产出形式	微晶颗粒，散布于水柱和沉积物	热液羽微颗粒、烟囱体、结壳、海底热液网脉	弥散的重晶石微颗粒，或胶结物、结核、透镜、薄层条带状	烟囱体、丘体、海底结壳，胶结物、结核、层状等
沉积或构造环境	非特定海域(高生产力海区更为显著)	热液喷流及热液羽区域，常见于洋中脊、弧后盆地等扩张中心、断裂带，陆架边缘断裂带，以及克拉通内部裂谷区等	高生产力海区(如陆架边缘上升流地区)	高生产力海区、陆架边缘陆坡带、构造及断层发育的主动、被动大陆边缘及复杂构造背景的海盆
生物群落	浮游生物、原生动物 xenophyophore 等	热液生物群		冷泉生物群
代表性伴生矿物	无特定伴生矿物	多金属硫化物、非晶质硅质沉积等	富有机质沉积物，黄铁矿、方解石、白云石等	黄铁矿、方解石、白云石等
粒度	亚微米级晶粒(普遍 $<5\mu m$)	数十至数百微米，可达毫米级	数十至数百微米，可达厘米级	数十至数百微米，可达厘米级
晶体形态	常为哑铃形、椭球形晶型，或不具有晶体习性	自形、棱柱形、板片状等晶型，放射针束状、扇状自形晶集合体，或者玫瑰花状结构	片状板柱状等自形晶型，有时可见交切板状双晶，以及树枝状、玫瑰状集合体	螺旋状、菱柱等晶型，以及树枝状和结核环带等生长模式；有时可见交切板状双晶和玫瑰花状结构
S 同位素	近似同时期海水值($\Delta\delta^{34}S\approx0$)	常介于同时期海水值与热液硫化物值之间($\Delta\delta^{34}S<0$)，但有时 $\Delta\delta^{34}S>0$	较同时期海水值不同程度偏高($\Delta\delta^{34}S>0$，可达+50‰)	较同时期海水值不同程度偏高($\Delta\delta^{34}S>0$，可达+50‰)
Sr 同位素	近似同时期海水值($\Delta^{87}Sr/^{86}Sr\approx0$)	显著偏离同时期海水值(通常 $-0.006<\Delta^{87}Sr/^{86}Sr<-0.002$；或 $\Delta^{87}Sr/^{86}Sr>+0.002$)	稍微偏离同时期海水值(通常 $-0.002<\Delta^{87}Sr/^{86}Sr<+0.002$)	稍微偏离同时期海水值(通常 $-0.002<\Delta^{87}Sr/^{86}Sr<+0.002$)
地质意义	记录海水 Sr、S 同位素组成，重建海洋生产力	指示热液活动、并记录热液流体化学特征，指导伴生的沉积喷流矿床的勘探	指示 SMTZ 和下伏甲烷输入，反映沉积速率变化，制约钡古生产力指标	指示甲烷释放和冷泉渗流事件，可能影响局部海域 Ba(和/或碳)循环，指导层状重晶石勘探

注：$\Delta\delta^{34}S=\delta^{34}S_{重晶石}-\delta^{34}S_{同时期海水硫酸盐}$；$\Delta^{87}Sr/^{86}Sr={}^{87}Sr/^{86}Sr_{重晶石}-{}^{87}Sr/^{86}Sr_{同时期海水}$

或深度而调节身体密度，海洋部分底栖原生动物(如有孔虫类 xenophyophore)可直接在细胞内生成重晶石[55-56]。另一方面，培养实验显示，海洋细菌能够提供晶体成核点并促进重晶石晶体的生长[57-58]。目前而言，这类海洋生物报道数量或实例有限，有待进一步探索；它们可能对整个重晶石储库的贡献份额有限。

另一方面，有机质降解时的微环境可促进重晶石的形成。许多海洋浮游生物直接从周围海水吸收钡进入生物结构，较海水相对富集钡[59]。例如，等幅骨虫(Acantharians)壳体由天青石($SrSO_4$)构成，常含有数千 ppm 的 Ba[60]。因此，它们含有相当规模的活性钡储库，在水柱里降解时可向临近微环境提供钡源，促进重晶石的形成[20,35,54]。例如，Ganeshram *et al.*[61]发现，海岸浮游生物以及实验室培养的硅藻和颗石藻在降解实验中可沉淀重晶石。此外，Dehairs *et al.*[62]推测，富有机质沉降颗粒里高强度细菌活动可能有助于海洋中层水柱高含量钡颗粒的生成。然而由于现今海洋处于重晶石未饱和状态，浮游生物降解时释放的钡能否被有效维存于微环境，对于重晶石沉淀至关重要[61]。目前认为，粪球粒和有机质团块等，虽然不是重晶石沉淀的必要条件，但能显著促进重晶石的生成[20,61]。理论上只要存在有机质集合体，重

晶石可以生成于任何水深,甚至沉积物—水界面附近[63]。

生物重晶石生成于水柱,呈现亚微米级晶粒(普遍<5 μm),常为哑铃形、椭球形晶型,或者不具有晶体习性[36,54,57]。由于形成于水柱,生物重晶石 Sr、S 和 O 同位素主要记录了同时期海水的特征,并可用于重建海水组分的长期演化趋势[17-19,49,64]。现今海洋水柱溶解 Ba 含量与重晶石颗粒和有机碳含量,以及上覆海水的生物生产力具有显著相关性,表明生物或有机质降解控制着水柱 Ba 循环[21,65-69]。因此,远洋氧化环境沉积物里生物重晶石与表层生物生产力之间存在显著的相关性[21],据此可作为重建海洋生物生产力的指标[20,22,70-71]。然而值得注意的是,在硫酸盐亏损的缺氧海水或沉积物孔隙水中(由于细菌硫酸盐还原作用),重晶石可能会经历不同程度的溶解;这种背景下沉积物里的 Ba 含量并不能有效指示海洋的初始生产力。

2.2　热液重晶石

热液重晶石是指深部富钡热流体沿断层或裂隙向海底运移或喷发至水柱过程中,与富硫酸盐流体相互作用而生成的重晶石(图 1B)[50,72-73]。热液流体里的钡离子可淋滤自洋壳、陆壳基底或长英质岩石(尤其是长石)、或者远洋富钡沉积物[50]。热液重晶石常源于火山岛弧、洋脊、弧后盆地扩张中心的岩浆热源驱动的富硫化物中高温集中流体(150℃~250℃)或中低温弥散流体(<120℃)的活动,如东北太平洋布兰科(Blanco)断裂带[74]、冲绳海槽 JADE 热液区[75]、北冰洋洋中脊南部 Loki's Castle 热液区[52]、马里亚纳岛弧[72,76-77]、克马德克岛弧[78-79]、汤加岛弧[80]、巴布亚新几内亚的富兰克林(Franklin)海山[73]、以及加那利群岛亨利(Henry)海山[81]。此外,在构造和减薄地壳导致的高热流背景下,陆架边缘的中低温热液流体也可发育热液重晶石,如南加利福尼亚大陆边缘[50]。

由于热流体运移速率差异,热液重晶石具有多种产出形式:①网脉状充填于海底面之下的热液通道[75],②在海底面之上形成烟囱体、丘体或结壳[72-73,77,82],③以细小颗粒形式随热液羽飘散,并散布于沉积物中[83-85]。洋脊或弧后扩张中心火山热液系统里的重晶石常伴生多金属硫化物(方铅矿、闪锌矿、黄铜矿、黄铁矿等)和非晶质硅质沉积[72-73,78,86]。克拉通内部裂谷或者陆架边缘的热液系统沉积的重晶石既可与块状硫化物矿床共生,也可伴生于块状硫化物矿床上部或毗邻区,形成独立的沉积型重晶石矿床,如阿拉斯加地区的 Red Dog 矿床[87]。热液重晶石呈现自形(如棱柱形、板片状等)晶型,粒度较大,为数十微米至毫米级。它们有时生长于开阔孔洞,构成放射针束状、扇状自形晶集合体[77],或者玫瑰花状结构[49]。

热液重晶石的生成常源于热液端元流体(热液成因 H_2S 氧化而来的硫酸盐 $\delta^{34}S$ 值为+1‰至+2‰)与海水(现今海水硫酸盐 $\delta^{34}S$ 值约为+20‰)不同程度的混合,因此具有不同程度偏低或类似于同时期海水硫酸盐的 $\delta^{34}S$ 值[49,88-89]。值得注意的是,如果上覆局限盆地海水或者海底热液系统里的硫酸盐处于相对封闭环境(即硫酸盐补充不足)时,细菌硫酸盐还原作用可使残余硫酸盐的硫同位素值不断增高。在此背景下,部分热液重晶石也可能具有较同时期海水值偏重的 $\delta^{34}S$ 值[52,75,81,90]。由于受到热液活动的影响,热液重晶石 $^{87}Sr/^{86}Sr$ 同位素值通常不同程度偏离同时期海水值,记录了热液流体淋滤洋壳或者陆壳的特征[91-92]。洋脊扩张中心和洋脊翼部的热液重晶石的 $^{87}Sr/^{86}Sr$ 值通常介于同时期海水值(现今海水 $^{87}Sr/^{86}Sr$ = 0.709 17)与萃取自洋壳的端元热液流体值($^{87}Sr/^{86}Sr$ = 0.703 05)之间[51];而克拉通内部裂谷或者陆架边缘的沉积喷流型热液重晶石则常具有高于同时期海水值的壳源 Sr 同位素特征[45,47]。

沉积物里热液重晶石的发育,指示存在热液活动,有助于加深对古海洋的认识。此外,热液重晶石是获取 Sr、S 同位素及流体包裹体测温的理想对象[75],可用于解析热液流体地球化学性质。因此,作为海底火山型块状硫化物矿床及沉积喷流型矿床里常见的伴生矿物,热液重晶石有助于认识相应的成矿过程,并促进硫化物矿床的勘探[87,90]。

2.3　成岩重晶石

成岩重晶石是指沉积物—水界面之下,原生生物重晶石在硫酸盐亏损带溶解后形成富钡孔隙水,迁移至硫酸盐—甲烷转换带(Sulfate-methane transition zones,SMTZ)附近与孔隙水残余硫酸盐相互作用而再沉淀的重晶石(图 1C)[24,38,93-95]。通常随着深度的增加,沉积物孔隙水里的硫酸盐由于来自上覆海水的扩散补充受限,并且经细菌硫酸盐还原作用而不断消耗[96-98]。随着硫酸盐的完全耗尽,沉积物里有机质在产甲烷细菌作用下进一步发酵产生甲烷,该区带称为产甲烷带(methanogenesis zone)。因此,沉积物—水界面之下一定深度可形成硫酸盐—甲烷转换带。

SMTZ之上为硫酸盐还原带,孔隙水含有硫酸盐,重晶石矿物性质稳定。SMTZ之下为产甲烷带,硫酸盐完全亏损,重晶石矿物将逐渐溶解,使得孔隙水具有高含量溶解钡[38,93,99]。SMTZ附近甲烷和硫酸盐近完全亏损,存在一个陡变的钡离子梯度(图1C)。下伏富钡(和甲烷)孔隙水向上扩散迁移,在SMTZ附近与向下扩散的残余硫酸盐汇合,导致形成自生成岩重晶石前锋带[38,93]。成岩重晶石前锋在现今水深数百米至上千米的海洋沉积物里时有发育,如环太平洋陆架边缘[38]、墨西哥湾[53]、美国东南海岸Blake Ridge[24,99]、纳米比亚陆架[93]、以及黑海[100]等地。

成岩重晶石的富集程度取决于SMTZ在特定深度的持续时间及溶解钡的输入情况。这又受到沉积速率[101]、下伏甲烷输入量[24]、沉积物里原生海洋生物重晶石含量等因素的影响[99]。通常,高生产力海区沉积物里可积累较丰富的生物重晶石,其大量溶解后有助于提升孔隙水钡离子含量,促进成岩重晶石的形成[38,94]。因此,成岩重晶石在富有机质岩层里更为常见。它们以弥散状重晶石晶粒、厘米至分米级重晶石结核或者薄层重晶石条带等多种形式产出[7,102-103]。由于具有相对稳定的生长条件,成岩重晶石常形成片状、板柱状等自形晶型,有时可见交切板状双晶,粒度常为数十至数百微米,有时可达厘米级[48-49]。它们可呈现树形生长、玫瑰状集合体等形态结构[38]。由于SMTZ里发育甲烷厌氧氧化作用(AOM),成岩重晶石可能也伴生黄铁矿、方解石、白云石等矿物[95,104-105]。

成岩重晶石形成于沉积物,主要记录了孔隙水Sr、S同位素特征。孔隙水环境里,细菌硫酸盐还原作用(BSR)优先将富^{32}S硫酸盐还原为H_2S,导致残余硫酸盐逐渐富集^{34}S(Rayleigh分馏效应)[97,106-107]。由于记录了孔隙水残余硫酸盐重硫同位素特征,成岩重晶石较同时期海水不同程度的富集^{34}S($\Delta\delta^{34}$S可达+50‰)[49,103]。另一方面,沉积柱中孔隙水主要继承或扩散自上覆海水,二者^{87}Sr/^{86}Sr值通常比较接近。但如果存在早期海洋沉积物、富放射性成因Sr的陆源物质及亏损^{87}Sr的洋壳物质等的改造时,孔隙水Sr同位素将不同程度的偏离同时期海水值[27,108]。因此,成岩重晶石的^{87}Sr/^{86}Sr反映了孔隙水与各种沉积物质的相互作用,接近或小幅度偏离同时期海水值(Δ^{87}Sr/^{86}Sr介于±0.002)[49,51]。

成岩重晶石及其富集情况能够指示烃类输入和SMTZ的位置[24,93,95,109-111],以及沉积速率显著变化[101]等地质过程。此外,成岩重晶石的发育,表明沉积物里的生物重晶石经历了溶解、迁移和再沉淀,这将制约钡含量在古生产力指标方面的应用[20,30,94]。值得注意的是,成岩重晶石及相关矿化作用在前寒武纪仅有少量报道[112-113],至显生宙其丰度和规模则有显著增加[16,90,101-103,105,111,114-115]。因此最近研究认为,这种情形可能响应了埃迪卡拉纪—寒武纪转折时期古海洋硫酸盐浓度及生态系统的转变[7]。

2.4 冷泉重晶石

冷泉重晶石是指富钡(或/和烃类)孔隙水沿裂隙运移至沉积物—水界面附近(冷泉渗流地),与富硫酸盐孔隙水或海水相互作用而形成的重晶石(图1D)[25-27,51,116]。冷泉重晶石与成岩重晶石在流体来源、沉积过程、同位素组成等多方面具有相似性。在断层、侧向挤压构造作用或者高沉积速率形成的沉积加载下,孔隙水可获得超压并垂向向上迁移。这将导致位于沉积物SMTZ里的成岩重晶石前锋带迁移至沉积物—水界面附近,转化为冷泉重晶石体系(图1C和D)[26,51,53]。冷泉流体的钡源与成岩重晶石类似,主要为沉积物里堆积的活性生物重晶石[51];因此冷泉重晶石常出现在高生产力背景下的富有机质沉积环境。冷泉重晶石在现今海洋时有报道,如加尼福尼亚陆架[27,116]、秘鲁陆架上升流地区[117]、阿拉斯加附近阿留申海槽[118]等汇聚型大陆架边缘,墨西哥湾[25,119]等被动大陆边缘,以及鄂霍兹克海[26]、日本海[120]等复杂构造背景的大陆边缘。此外,墨西哥、中国南方、美国阿拉斯加和内华达地区古生代大型层状重晶石矿床[51],以及非洲西北部Taoudéni Basin新元古代盖帽碳酸盐岩里的重晶石沉积等也被认为与冷泉活动有关[121]。

冷泉重晶石的产出形式受制于重晶石前锋带的深度(图1D),而这又受控于冷泉流体渗流速率[23,53]:低渗流速率时,重晶石沉积于沉积物—水界面附近的孔隙环境,形成微晶胶结物或结核(类似成岩重晶石);高渗流速率时,重晶石沉积于海底面或水柱,形成结壳、多孔丘体以及大型烟囱体等典型的冷泉渗流结构[25-27,116,119]。冷泉重晶石呈现螺旋状、菱柱状等晶型,可见交切板状双晶;有时形成玫瑰花状、树枝状和结核环带等生长模式[26,119-120]。由于常伴生AOM作用,冷泉重晶石沉积常可共生碳酸盐岩及少量黄铁矿。其中,重晶石和碳酸盐岩的相对含量受控于孔隙水里甲烷与钡离子含量的比例[23]:低甲烷/钡离子比值条件下,以重晶石沉淀为主;高比值条

件下,硫酸盐受到AOM的消耗,以碳酸盐岩沉淀为主。因此,冷泉重晶石和冷泉碳酸盐岩普遍共生,但也可以相互独立而存在[51,90]。值得注意的是,现今海底冷泉重晶石沉积区也可能伴生相应的冷泉生物群,如微生物席,以及贝类、管状蠕虫、腹足等大型生物[25-27,118]。

冷泉重晶石的Sr和S同位素主要记录了孔隙水与海水的混合信号。若海水混合比例较低时,冷泉重晶石与成岩重晶石具有相似的孔隙水Sr、S同位素特征,即与同时期海水值相比具有相近的$^{87}Sr/^{86}Sr$比值($\Delta^{87}Sr/^{86}Sr$介于±0.002),以及显著偏重的$\delta^{34}S$值[15,49,51]。若海水混合显著时,冷泉重晶石的Sr、S同位素将更为接近同时期海水值。需要指出的是,冷泉重晶石的$\delta^{34}S/\delta^{18}O$比值可提供渗流速率和硫酸盐还原速率信息:该值大于4∶1(代表微生物硫酸盐还原作用斜率值)被认为指示了低渗流速率背景下高微生物硫酸盐还原速率(硫酸盐相对封闭体系),反之则指示高渗流速率背景下低微生物还原速率(硫酸盐相对开放体系)[25]。

冷泉是陆架边缘重要的地质过程,其释放大量低温富钡(和甲烷流体)流体,可能显著影响半封闭海洋盆地[116,122],甚至地质历史时期全球海洋钡(和碳)循环[28]。此外,地质历史里的冷泉重晶石也直接指示甲烷输入和冷泉渗流事件[109,123-125],并可能是古生代层状重晶石矿床的成因机制[15,51,126]。

3　扬子地区下寒武统重晶石

华南扬子地区下寒武统黑色页岩—硅质岩地层普遍富含重晶石,具有显著的高钡含量特征(常高于1 000 ppm,有时甚至可达数万ppm)[127-128]。其中,扬子地区湘黔相邻区牛蹄塘组和秦岭大巴山地区洞河群发育大型层状重晶石成矿带,是沉积型重晶石矿床的典型代表[1,47,129-132]。重晶石在沉积物里异常富集,通常需要特殊的地质条件(如高生产力背景下生物重晶石或者富钡流体的大量输入等)[133],而这通常反映了重要的地质事件。在此,我们以扬子地区下寒武统重晶石为例,分析其沉积特征,讨论富集机制和地质意义。

3.1　地质特征

扬子地区下寒武统富重晶石岩系在地理图上呈带状分布[129,132]。基于主微量等地球化学特征,目前普遍认为下寒武统富重晶石的黑色岩系主要沉积于缺氧环境[132,134-137]。重晶石矿床的硫酸钡含量一般为85%~95%,并伴生毒重石、钡解石、黄铁矿、钡冰长石、斜钡钙石、闪锌矿、硫钒铜矿和胶磷矿等矿物[130,138]。重晶石呈现弥散、层状、透镜状、条带状、结核状、玫瑰花状等多种沉积结构。重晶石围岩里可见藻类、海绵骨针、管状生物等化石[139]。同位素地球化学方面,层状重晶石$\delta^{34}S$值一般为+25‰至+60‰[132,138,140-143],其中重晶石结核$\delta^{34}S$值可达74‰[103];较早寒武世海水(35‰~40‰)[144]显著富集^{34}S。扬子地区下寒武统重晶石$^{87}Sr/^{86}Sr$分布较窄,普遍介于0.708 0至0.709 0之间[132,145-146],总体接近早寒武世海水值(0.708 2~0.709 0)[147]。少量重晶石样品可能受陆源杂质的影响,$^{87}Sr/^{86}Sr$比值可达0.709 5~0.716 7[146]。

3.2　富集机制

根据下寒武统重晶石富集的地质特征,研究者们提出了多种成因机制,如生物富集[1,148]、富钡冷泉流体释放[15,51]、或者热液活动[47,129-130,142,145,149]等地质作用。

生物富集模式支持者认为,早寒武世扬子地区陆架边缘上升流发育,富营养水体促进生物繁盛,高生产力背景下生成大量海洋生物重晶石[1,148]。它们可能直接导致层状重晶石的沉积,或者在缺氧海盆或沉积物里经溶解、迁移再沉淀形成富重晶石沉积。该模式得到重晶石及其围岩(黑色页岩—硅质岩)富含有机质、Si和P元素证据的支持,暗示沉积时水柱处于高生产力背景或者缺氧环境[137,149]。然而,重晶石的Sr、S同位素特征均不同程度偏离同时期海水值,这显著不同于水柱直接生成的生物成因重晶石。同时,单一的生物作用模式难以解释扬子地区下寒武统重晶石富集的形态、规模和品位,且缺乏古今实例。

冷泉作用模式认为,扬子地区下寒武统大型层状重晶石沉积可能受益于陆架边缘富钡(和烃)的冷泉活动[15,51,132]。扬子地区下寒武统重晶石的Sr同位素比值在同时期海水值附近小幅度波动[146],表明可能源于受沉积物改造的孔隙水。它们的硫同位素较同时期海水显著偏重[140],可能记录了沉积物孔隙水里残余硫酸盐(富集^{34}S同位素)的信号。因此,下寒武统重晶石的Sr和S同位素特征与现今成岩或冷泉重晶石相似[51,132]。此外,下寒武统重晶石富集的冷泉模式也得到其他地质证据的支持:①重晶石具有成岩和海底生长特征[139],表明随着孔隙水流体向上运移强弱的变化,重晶石前锋带深度不断波动;②围岩里的化石疑似冷泉生物群;③牛蹄塘组早成岩重晶

石—黄铁矿结核显示沉积物里发育冷泉流体[103]；④重晶石未见伴生的大规模的贱金属硫化物沉积；⑤富重晶石沉积带状分布，表明受控于断层相关的冷泉流体通道；⑥现今大陆边缘可见冷泉重晶石显著富集的实例[51,117]。值得注意的是，扬子地区下寒武统部分重晶石（毒重石）也不同程度经历了早成岩作用的富集[103,132]。

热液活动模式认为，前寒武纪—寒武纪转折时期扬子地区广泛发育海底热液活动[128,150]，并促进了下寒武统硅质岩和Ni-Mo多金属的沉积[151]。在此背景下，下寒武统重晶石富集也可能源于热液活动，并得到大量地质证据的支持：①重晶石具有网脉结构及热水喷流沉积结构[130]；②硅质岩、黑色页岩等重晶石围岩的地球化学特征显示有热液流体的影响[142,152]；③重晶石Sr同位素值偏离同时期海水值，反映了热液流体的贡献[47,129,145-146]；④伴生少量黄铜矿、环带钡冰长石等热液矿物[135,153-154]；⑤流体包裹体数据揭示中等温度条件[131]；⑥围岩里的化石疑似海底热液生物群[139]；⑦重晶石成矿带线性排列，表明似乎受控于断层相关的热液流体通道。

3.3 讨论

由此可见，扬子地区下寒武统重晶石的各种富集机制均能得到地质证据不同程度的支持。然而，有些证据并非特定成因模式的必要条件。比如，重晶石较海水显著较重的$\delta^{34}S$值，显示了在硫酸盐亏损环境里、微生物硫酸盐还原的分馏作用。这种环境可能是海洋生物富集模式里硫酸盐供给不足的局限海盆环境[129,135,140,143]，也可以是冷泉模式里海洋沉积物中的孔隙水环境[15,132]。同时，重晶石Sr同位素相对于早寒武世海水值一定程度的偏移，也分别被解释为热液[135,145]，或者海水来源的证据[132]。另一方面，扬子地区下寒武统重晶石富集带的线性分布特征，既可能是受控于陆架边缘沿岸上升流高生产力条件，也可能受控于断层相关的冷泉或热液流体通道。此外，重晶石富集带是否伴生硫化物矿床、是否发育烃类流体及相关的碳酸盐岩沉积、渗（喷）流流体温度特征及Sr同位素解释等，也可以是冷泉模式和热液模式的重要分歧[51,91,151]。

因此，扬子地区下寒武统重晶石的显著富集可能涉及各种成因过程。例如，高生产力背景下，陆架边缘沉积物里初步富集海洋生物重晶石。早成岩阶段，这些重晶石不断溶解，提升孔隙流体钡含量，一方面可迁移至SMTZ附近再沉淀而不断富集，另一方面也可为冷泉或热液重晶石提供钡源。反之，大量富钡冷泉或热液流体释放至海水，也可能促进水柱里海洋（生物）重晶石的生成。值得注意的是，埃迪卡拉纪—寒武纪转折时期海洋生态（后生动物及粪球粒的到来）[155-156]，以及海洋地球化学（硫酸盐浓度的增高）[157]的转变，可能是理解下寒武统普遍具有高钡含量及富集重晶石的一个新思路[7]。总之，扬子地区下寒武统黑色岩系富重晶石沉积的成因机制仍然悬而未决。结合该时期古海洋背景，在详细的沉积学基础上，综合地球化学特征，有助于深化对该层段重晶石的沉积类型和成因机制的认识，并弥合分歧。

4 结论

沉积型重晶石在地质历史里分布广泛、类型丰富，具有重要的经济和地质意义。基于形成环境、宏微观沉积特征、Sr和S同位素组成等特点，沉积型重晶石可分为生物、热液、成岩和冷泉重晶石四个端元类型。通过地质特征，识别重晶石成因类型，是合理解读相应地质意义的关键。扬子地区下寒武统重晶石不同程度体现了生物、冷泉（及成岩）和热液重晶石的地质特征，相关研究有待进一步深化。

参考文献（References）

1 Jewell P W. Bedded barite in the geologic record[M]//Glenn C R, Prévôt L, Lucas J. Marine Authigenesis: from Global to Microbial. Society Economic Paleontologists Mineralogists Special Publication, 2000, 66(1): 147-161.

2 Hanor J S. Barite-celestine geochemistry and environments of formation[J]. Reviews in Mineralogy and Geochemistry, 2000, 40(1): 193-275.

3 Shen Yanan, Buick R, Canfield D E. Isotopic evidence for microbial sulphate reduction in the early Archaean era[J]. Nature, 2001, 410(6824): 77-81.

4 McClung C R, Gutzmer J, Beukes N J, et al. Geochemistry of bedded barite of the Mesoproterozoic Aggeneys-Gamsberg Broken Hill-type district, South Africa[J]. Mineralium Deposita, 2007, 42(5): 537-549.

5 Lyons T W, Gellatly A M, McGoldrick P J, et al. Proterozoic sedimentary exhalative (SEDEX) deposits and links to evolving global ocean chemistry[J]. Geological Society of America Memoirs, 2006, 198: 169-184.

6 Huston D L, Logan G A. Barite, BIFs and bugs: evidence for the evolution of the Earth´s early hydrosphere[J]. Earth and Planetary Science Letters, 2004, 220(1/2): 41-55.

7 Zhou Xiqiang, Chen Daizhao, Dong Shaofeng, et al. Diagenetic barite deposits in the Yurtus Formation in Tarim Basin, NW China: implications for barium and sulfur cycling in the earliest Cambrian[J]. Precambrian Research, 2015, 263: 79-87.

8 Peng Yongbo, Bao Huiming, Zhou Chuanming, et al. Oxygen isotope composition of meltwater from a Neoproterozoic glaciation in South China[J]. Geology, 2013, 41(3): 367-370.

9 Killingsworth B A, Hayles J A, Zhou Chuanming, et al. Sedimentary constraints on the duration of the Marinoan Oxygen-17 Depletion (MOSD) event[J]. Proceedings of the National Academy of Sciences of the United States of America, 2013, 110(44): 17686-17690.

10 Peng Yongbo, Bao Huiming, Zhou Chuanming, et al. ^{17}O-depleted barite from two Marinoan cap dolostone sections, South China[J]. Earth and Planetary Science Letters, 2011, 305(1/2): 21-31.

11 Zhou Chunming, Bao Huiming, Peng Yongbo, et al. Timing the deposition of ^{17}O-depleted barite at the aftermath of Nantuo glacial meltdown in South China[J]. Geology, 2010, 38(10): 903-906.

12 Bao Huiming, Rumble III D, Lowe D R. The five stable isotope compositions of Fig Tree barites: implications on sulfur cycle in ca. 3.2 Ga oceans[J]. Geochimica et Cosmochimica Acta, 2007, 71(20): 4868-4879.

13 Staude S, Göb S, Pfaff K, et al. Deciphering fluid sources of hydrothermal systems: a combined Sr- and S-isotope study on barite (Schwarzwald, SW Germany)[J]. Chemical Geology, 2011, 286(1/2): 1-20.

14 Shen Yanan, Farquhar J, Masterson A, et al. Evaluating the role of microbial sulfate reduction in the early Archean using quadruple isotope systematics[J]. Earth and Planetary Science Letters, 2009, 279(3/4): 383-391.

15 Johnson C A, Emsbo P, Poole F G, et al. Sulfur- and oxygen-isotopes in sediment-hosted stratiform barite deposits[J]. Geochimica et Cosmochimica Acta, 2009, 73(1): 133-147.

16 Magnall J M, Gleeson S A, Stern R A, et al. Open system sulphate reduction in a diagenetic environment-isotopic analysis of barite (δ^{34}S and δ^{18}O) and pyrite (δ^{34}S) from the Tom and Jason Late Devonian Zn-Pb-Ba deposits, Selwyn Basin, Canada[J]. Geochimica et Cosmochimica Acta, 2016, 180: 146-163.

17 Paytan A, Kastner M, Campbell D, et al. Sulfur isotopic composition of Cenozoic seawater sulfate[J]. Science, 1998, 282(5393): 1459-1462.

18 Paytan A, Kastner M, Martin E E, et al. Marine barite as a monitor of seawater strontium isotope composition[J]. Nature, 1993, 366(6454): 445-449.

19 Bottrell S H, Newton R J. Reconstruction of changes in global sulfur cycling from marine sulfate isotopes[J]. Earth-Science Reviews, 2006, 75(1/2/3/4): 59-83.

20 Paytan A, Griffith E M. Marine barite: recorder of variations in ocean export productivity[J]. Deep Sea Research Part II: Topical Studies in Oceanography, 2007, 54(5/6/7): 687-705.

21 Dymond J, Suess E, Lyle M. Barium in deep-sea sediment: a geochemical proxy for paleoproductivity[J]. Paleoceanography, 1992, 7(2): 163-181.

22 Schoepfer S D, Shen Jun, Wei Hengye, et al. Total organic carbon, organic phosphorus, and biogenic barium fluxes as proxies for paleomarine productivity[J]. Earth-Science Reviews, 2015, 149: 23-52.

23 Aloisi G, Wallmann K, Bollwerk S M, et al. The effect of dissolved barium on biogeochemical processes at cold seeps[J]. Geochimica et Cosmochimica Acta, 2004, 68(8): 1735-1748.

24 Dickens G R. Sulfate profiles and barium fronts in sediment on the Blake Ridge: present and past methane fluxes through a large gas hydrate reservoir[J]. Geochimica et Cosmochimica Acta, 2001, 65(4): 529-543.

25 Feng Dong, Roberts H H. Geochemical characteristics of the barite deposits at cold seeps from the northern Gulf of Mexico continental slope[J]. Earth and Planetary Science Letters, 2011, 309(1/2): 89-99.

26 Greinert J, Bollwerk S M, Derkachev A, et al. Massive barite deposits and carbonate mineralization in the Derugin Basin, Sea of Okhotsk: precipitation processes at cold seep sites[J]. Earth and Planetary Science Letters, 2002, 203(1): 165-180.

27 Naehr T H, Stakes D S, Moore W S. Mass wasting, ephemeral fluid flow, and barite deposition on the California continental margin[J]. Geology, 2000, 28(4): 315-318.

28 Dickens G R, Fewless T, Thomas E, et al. Excess barite accumulation during the Paleocene-Eocene thermal Maximum: Massive input of dissolved barium from seafloor gas hydrate reservoirs[J]. Geological Society of America Special Papers, 2003, 369: 11-23.

29 Gonneea M E, Paytan A. Phase associations of barium in marine sediments[J]. Marine Chemistry, 2006, 100(1/2): 124-135.

30 McManus J, Berelson W M, Klinkhammer G P, et al. Geochemistry of barium in marine sediments: implications for its use as a paleoproxy[J]. Geochimica et Cosmochimica Acta, 1998, 62(21/22): 3453-3473.

31 Monnin C. A thermodynamic model for the solubility of barite and celestite in electrolyte solutions and seawater to 200°C and to 1 kbar[J]. Chemical Geology, 1999, 153(1/2/3/4): 187-209.

32 Monnin C, Cividini D. The saturation state of the world´s ocean with respect to (Ba,Sr)SO_4 solid solutions[J]. Geochimica et Cosmochimica Acta, 2006, 70(13): 3290-3298.

33 Monnin C, Jeandel C, Cattaldo T, et al. The marine barite saturation state of the world´s oceans[J]. Marine Chemistry, 1999, 65(3/4): 253-261.

34 Rushdi A I, McManus J, Collier R W. Marine barite and celestite saturation in seawater[J]. Marine Chemistry, 2000, 69(1/2): 19-31.

35 Bishop J K B. The barite-opal-organic carbon association in oceanic particulate matter[J]. Nature, 1988, 332(6162): 341-343.

36 Dehairs F, Chesselet R, Jedwab J. Discrete suspended particles of barite and the barium cycle in the open ocean[J]. Earth and Planetary Science Letters, 1980, 49(2): 528-550.

37 McManus J, Berelson W M, Klinkhammer G P, et al. Remobilization of barium in continental margin sediments[J]. Geochimica et Cosmochimica Acta, 1994, 58(22): 4899-4907.

38 Torres M E, Brumsack H J, Bohrmann G, et al. Barite fronts in continental margin sediments: a new look at barium remobilization in the zone of sulfate reduction and formation of heavy barites in diagenetic fronts[J]. Chemical Geology, 1996, 127(1/2/3): 125-139.

39 Steele J H, Thorpe S A, Turekian K K. Encyclopedia of Ocean Sciences[M]. 2nd ed. Amsterdam: Academic Press, 2011: 255-260.

40 Falkner K K, Klinkhammer G P, Bowers T S, et al. The behavior of barium in anoxic marine waters[J]. Geochimica et Cosmochimica Acta, 1993, 57(3): 537-554.

41 Coffey M, Dehairs F, Collette O, et al. The behaviour of dissolved barium in estuaries[J]. Estuarine, Coastal and Shelf Science, 1997, 45(1): 113-121.

42 Stecher III H A, Kogut M B. Rapid barium removal in the Delaware estuary[J]. Geochimica et Cosmochimica Acta, 1999, 63(7/8): 1003-1012.

43 Douville E, Charlou J L, Oelkers E H, et al. The rainbow vent fluids (36°14′N, MAR): the influence of ultramafic rocks and phase separation on trace metal content in Mid-Atlantic Ridge hydrothermal fluids [J]. Chemical Geology, 2002, 184(1/2): 37-48.

44 Elderfield H, Schultz A. Mid-ocean ridge hydrothermal fluxes and the chemical composition of the ocean[J]. Annual Review of Earth and Planetary Sciences, 1996, 24(1): 191-224.

45 Maynard J B, Morton J, Valdes-Nodarse E L, et al. Sr isotopes of bedded barites; guide to distinguishing basins with Pb-Zn mineralization[J]. Economic Geology, 1995, 90(7): 2058-2064.

46 Maynard J B, Okita P M. Bedded barite deposits in the United States, Canada, Germany, and China; two major types based on tectonic setting[J]. Economic Geology, 1991, 86(2): 364-376.

47 Clark S H B, Poole F G, Wang Zhongcheng. Comparison of some sediment-hosted, stratiform barite deposits in China, the United States, and India[J]. Ore Geology Reviews, 2004, 24(1/2): 85-101.

48 Griffith E M, Paytan A. Barite in the ocean-occurrence, geochemistry and palaeoceanographic applications[J]. Sedimentology, 2012, 59(6): 1817-1835.

49 Paytan A, Mearon S, Cobb K, et al. Origin of marine barite deposits: Sr and S isotope characterization[J]. Geology, 2002, 30(8): 747-750.

50 Hein J R, Zierenberg R A, Maynard J B, et al. Barite-forming environments along a rifted continental margin, Southern California Borderland[J]. Deep Sea Research Part II: Topical Studies in Oceanography, 2007, 54(11/12/13): 1327-1349.

51 Torres M E, Bohrmann G, Dubé T E, et al. Formation of modern and Paleozoic stratiform barite at cold methane seeps on continental margins[J]. Geology, 2003, 31(10): 897-900.

52 Eickmann B, Thorseth I H, Peters M, et al. Barite in hydrothermal environments as a recorder of subseafloor processes: a multiple-isotope study from the Loki′s Castle vent field[J]. Geobiology, 2014, 12(4): 308-321.

53 Castellini D G, Dickens G R, Snyder G T, et al. Barium cycling in shallow sediment above active mud volcanoes in the Gulf of Mexico [J]. Chemical Geology, 2006, 226(1/2): 1-30.

54 Bertram M A, Cowen J P. Morphological and compositional evidence for biotic precipitation of marine barite[J]. Journal of Marine Research, 1997, 55(3): 577-593.

55 Gooday A J, Nott J A. Intracellular barite crystals in two xenophyophores, *Aschemonella ramuliformis* and *Galatheammina* sp. (Protozoa: Rhizopoda) with comments on the taxonomy of *A. ramuliformis*[J]. Journal of the Marine Biological Association of the United Kingdom, 1982, 62(3): 595-605.

56 Swinbanks D D, Shirayama Y. High levels of natural radionuclides in a deep-sea infaunal xenophyophore[J]. Nature, 1986, 320(6060): 354-358.

57 Gonzalez-Muñoz M T, Martinez-Ruiz F, Morcillo F, et al. Precipitation of barite by marine bacteria: A possible mechanism for marine barite formation[J]. Geology, 2012, 40(8): 675-678.

58 González-Munoz M T, Fernández-Luque B, Martínez-Ruiz F, et al. Precipitation of barite by *Myxococcus xanthus*: possible implications for the biogeochemical cycle of barium[J]. Applied and Environmental Microbiology, 2003, 69(9): 5722-5725.

59 Fisher N S, Guillard R R L, Bankston D C. The accumulation of barium by marine phytoplankton grown in culture[J]. Journal of Marine Research, 1991, 49(2): 339-354.

60 Bernstein R E, Byrne R H. Acantharians and marine barite[J]. Marine Chemistry, 2004, 86(1/2): 45-50.

61 Ganeshram R S, François R, Commeau J, et al. An experimental investigation of barite formation in seawater[J]. Geochimica et Cosmochimica Acta, 2003, 67(14): 2599-2605.

62 Dehairs F, Jacquet S, Savoye N, et al. Barium in twilight zone suspended matter as a potential proxy for particulate organic carbon remineralization: Results for the North Pacific[J]. Deep Sea Research Part II: Topical Studies in Oceanography, 2008, 55(14/15): 1673-1683.

63 van Beek P, François R, Conte M, et al. $^{228}Ra/^{226}Ra$ and $^{226}Ra/Ba$ ratios to track barite formation and transport in the water column[J]. Geochimica et Cosmochimica Acta, 2007, 71(1): 71-86.

64 Markovic S, Paytan A, Li Hong, et al. A revised seawater sulfate oxygen isotope record for the last 4Myr[J]. Geochimica et Cosmochimica Acta, 2016, 175: 239-251.

65 Dehairs F, Baeyens W, Goeyens L. Accumulation of suspended barite at mesopelagic depths and export production in the Southern Ocean [J]. Science, 1992, 258(5086): 1332-1335.

66 Dehairs F, Stroobants N, Goeyens L. Suspended barite as a tracer of biological activity in the Southern Ocean[J]. Marine Chemistry, 1991, 35(1/2/3/4): 399-410.

67 Dymond J, Collier R. Particulate barium fluxes and their relationships to biological productivity[J]. Deep Sea Research Part II: Topical Studies in Oceanography, 1996, 43(4/5/6): 1283-1308.

68 Cardinal D, Savoye N, Trull T W, et al. Variations of carbon remineralisation in the Southern Ocean illustrated by the Ba_{xs} proxy[J]. Deep Sea Research Part I: Oceanographic Research Papers, 2005, 52(2): 355-370.

69 Jeandel C, Tachikawa K, Bory A, et al. Biogenic barium in suspended and trapped material as a tracer of export production in the tropical NE Atlantic (EUMELI sites)[J]. Marine Chemistry, 2000, 71(1/2): 125-142.

70 Francois R, Honjo S, Manganini S J, et al. Biogenic barium fluxes to

the deep sea: implications for paleoproductivity reconstruction[J]. Global Biogeochemical Cycles, 1995, 9(2): 289-303.

71 Ma Zhongwu, Ravelo A C, Liu Zhonghui, et al. Export production fluctuations in the eastern equatorial Pacific during the Pliocene-Pleistocene: reconstruction using barite accumulation rates[J]. Paleoceanography, 2015, 30(11): 1455-1469.

72 Urabe T, Kusakabe M. Barite silica chimneys from the Sumisu Rift, Izu-Bonin Arc: possible analog to hematitic chert associated with Kuroko deposits[J]. Earth and Planetary Science Letters, 1990, 100(1/2/3): 283-290.

73 Binns R A, Parr J M, Gemmell J B, et al. Precious metals in barite-silica chimneys from Franklin Seamount, Woodlark Basin, Papua New Guinea[J]. Marine Geology, 1997, 142(1/2/3/4): 119-141.

74 Hein J R, Koski R A, Embley R W, et al. Diffuse-flow hydrothermal field in an oceanic fracture zone setting, Northeast Pacific: deposit composition[J]. Exploration and Mining Geology, 1999, 8(3/4): 299-322.

75 Lüders V, Pracejus B, Halbach P. Fluid inclusion and sulfur isotope studies in probable modern analogue Kuroko-type ores from the JADE hydrothermal field (Central Okinawa Trough, Japan)[J]. Chemical Geology, 2001, 173(1/2/3): 45-58.

76 Stüben D, Taibi N E, McMurtry G M, et al. Growth history of a hydrothermal silica chimney from the Mariana backarc spreading center (southwest Pacific, 18°13´N)[J]. Chemical Geology, 1994, 113(3/4): 273-296.

77 Moore W S, Stakes D. Ages of barite-sulfide chimneys from the Mariana Trough[J]. Earth and Planetary Science Letters, 1990, 100(1/2/3): 265-274.

78 Herzig P M, Becker K P, Stoffers P, et al. Hydrothermal silica chimney fields in the Galapagos spreading center at 86°W[J]. Earth and Planetary Science Letters, 1988, 89(3/4): 261-272.

79 de Ronde C E, Faure K, Bray C J, et al. Hydrothermal fluids associated with seafloor mineralization at two southern Kermadec arc volcanoes, offshore New Zealand[J]. Mineralium Deposita, 2003, 38(2): 217-233.

80 Stoffers P, Worthington T J, Schwarz-Schampera U, et al. Submarine volcanoes and high-temperature hydrothermal venting on the Tonga arc, southwest Pacific[J]. Geology, 2006, 34(6): 453-456.

81 Klügel A, Hansteen T H, van den Bogaard P, et al. Holocene fluid venting at an extinct Cretaceous seamount, Canary archipelago[J]. Geology, 2011, 39(9): 855-858.

82 Petersen S, Herzig P M, Schwarz-Schampera U, et al. Hydrothermal precipitates associated with bimodal volcanism in the Central Bransfield Strait, Antarctica[J]. Mineralium Deposita, 2004, 39(3): 358-379.

83 Mottl M J, McConachy T F. Chemical processes in buoyant hydrothermal plumes on the East Pacific Rise near 21°N[J]. Geochimica et Cosmochimica Acta, 1990, 54(7): 1911-1927.

84 Feely R A, Geiselman T L, Baker E T, et al. Distribution and composition of hydrothermal plume particles from the ASHES vent field at Axial Volcano, Juan de Fuca Ridge[J]. Journal of Geophysical Research, 1990, 95(B8): 12855-12873.

85 Peters M, Strauss H, Petersen S, et al. Hydrothermalism in the Tyrrhenian Sea: inorganic and microbial sulfur cycling as revealed by geochemical and multiple sulfur isotope data[J]. Chemical Geology, 2011, 280(1/2): 217-231.

86 Halbach M, Halbach P, Lüders V. Sulfide-impregnated and pure silica precipitates of hydrothermal origin from the central Indian Ocean[J]. Chemical Geology, 2002, 182(2/3/4): 357-375.

87 Kelley K, Jennings S. A special issue devoted to barite and Zn-Pb-Ag deposits in the Red Dog district, Western Brooks Range, Northern Alaska[J]. Economic Geology, 2004, 99(7): 1267-1280.

88 Rye R O. A review of the stable-isotope geochemistry of sulfate minerals in selected igneous environments and related hydrothermal systems[J]. Chemical Geology, 2005, 215(1/2/3/4): 5-36.

89 Herzig P M, Hannington M D, Arribas A, Jr. Sulfur isotopic composition of hydrothermal precipitates from the Lau back-arc: implications for magmatic contributions to seafloor hydrothermal systems[J]. Mineralium Deposita, 1998, 33(3): 226-237.

90 Johnson C, Kelley K, Leach D L. Sulfur and oxygen isotopes in barite deposits of the western Brooks Range, Alaska, and implications for the origin of the Red Dog massive sulfide deposits[J]. Economic Geology, 2004, 99(7): 1435-1448.

91 Emsbo P, Johnson C A. Formation of modern and Paleozoic stratiform barite at cold methane seeps on continental margins: comment and reply comment[J]. Geology, 2004, 32(1): e64.

92 Noguchi T, Shinjo R, Ito M, et al. Barite geochemistry from hydrothermal chimneys of the Okinawa Trough: insight into chimney formation and fluid/sediment interaction[J]. Journal of Mineralogical and Petrological Sciences, 2011, 106(1): 26-35.

93 Riedinger N, Kasten S, Gröger J, et al. Active and buried authigenic barite fronts in sediments from the Eastern Cape Basin[J]. Earth and Planetary Science Letters, 2006, 241(3/4): 876-887.

94 Hendy I L. Diagenetic behavior of barite in a coastal upwelling setting[J]. Paleoceanography, 2010, 25(4): PA4103.

95 Snyder G T, Hiruta A, Matsumoto R, et al. Pore water profiles and authigenic mineralization in shallow marine sediments above the methane-charged system on Umitaka Spur, Japan Sea[J]. Deep Sea Research Part II: Topical Studies in Oceanography, 2007, 54(11/12/13): 1216-1239.

96 Goldhaber M B, Kaplan I R. Mechanisms of sulfur incorporation and isotope fractionation during early diagenesis in sediments of the Gulf of California[J]. Marine Chemistry, 1980, 9(2): 95-143.

97 Canfield D E. Biogeochemistry of sulfur isotopes[J]. Reviews in Mineralogy and Geochemistry, 2001, 43(1): 607-636.

98 Jørgensen B B, Weber A, Zopfi J. Sulfate reduction and anaerobic methane oxidation in Black Sea sediments[J]. Deep Sea Research Part I: Oceanographic Research Papers, 2001, 48(9): 2097-2120.

99 Snyder G T, Dickens G R, Castellini D G. Labile barite contents and dissolved barium concentrations on Blake Ridge: new perspectives on barium cycling above gas hydrate systems[J]. Journal of Geochemical Exploration, 2007, 95(1/2/3): 48-65.

100 Henkel S, Mogollón J M, Nöthen K, et al. Diagenetic barium cycling in Black Sea sediments – a case study for anoxic marine environments[J]. Geochimica et Cosmochimica Acta, 2012, 88: 88-105.

101 Bréhéret J G, Brumsack H J. Barite concretions as evidence of pauses in sedimentation in the Marnes Bleues Formation of the Vocontian Basin (SE France)[J]. Sedimentary Geology, 2000, 130(3/4): 205-228.

102 Leśniak P M, Łącka B, Hladíkova J, et al. Origin of barite concretions in the West Carpathian flysch, Poland[J]. Chemical Geology, 1999, 158(1/2): 155-163.

103 Goldberg T, Mazumdar A, Strauss H, et al. Insights from stable S and O isotopes into biogeochemical processes and genesis of Lower Cambrian barite-pyrite concretions of South China[J]. Organic Geochemistry, 2006, 37(10): 1278-1288.

104 Moore T S, Murray R W, Kurtz A C, et al. Anaerobic methane oxidation and the formation of dolomite[J]. Earth and Planetary Science Letters, 2004, 229(1/2): 141-154.

105 Raiswell R, Bottrell S H, Dean S P, et al. Isotopic constraints on growth conditions of multiphase calcite – pyrite – barite concretions in Carboniferous mudstones[J]. Sedimentology, 2002, 49(2): 237-254.

106 Böttcher M E, Khim B K, Suzuki A, et al. Microbial sulfate reduction in deep sediments of the Southwest Pacific (ODP Leg 181, Sites 1119-1125): evidence from stable sulfur isotope fractionation and pore water modeling[J]. Marine Geology, 2004, 205(1/2/3/4): 249-260.

107 Borowski W S, Rodriguez N M, Paull C K, et al. Are ^{34}S-enriched authigenic sulfide minerals a proxy for elevated methane flux and gas hydrates in the geologic record? [J]. Marine and Petroleum Geology, 2013, 43: 381-395.

108 Dia A N, Aquilina L, Boulègue J, et al. Origin of fluids and related barite deposits at vent sites along the Peru convergent margin[J]. Geology, 1993, 21(12): 1099-1102.

109 Kasten S, Nöthen K, Hensen C, et al. Gas hydrate decomposition recorded by authigenic barite at pockmark sites of the northern Congo Fan[J]. Geo-Marine Letters, 2012, 32(5/6): 515-524.

110 Arndt S, Hetzel A, Brumsack H J. Evolution of organic matter degradation in Cretaceous black shales inferred from authigenic barite: a reaction-transport mode[J]. Geochimica et Cosmochimica Acta, 2009, 73(7): 2000-2022.

111 Niu D, Renock D, Whitehouse M, et al. A relict sulfate – methane transition zone in the mid-Devonian Marcellus Shale[J]. Geochimica et Cosmochimica Acta, 2016, 182: 73-87.

112 Heinrichs T, Reimer T. A sedimentary barite deposit from the Archean Fig Tree Group of the Barberton Mountain Land (South Africa) [J]. Economic Geology, 1977, 72(8): 1426-1441.

113 Reimer T O. Archean sedimentary baryte deposits of the Swaziland Supergroup (Barberton Mountain Land, South Africa)[J]. Precambrian Research, 1980, 12(1/2/3/4): 393-410.

114 Lash G G. Authigenic barite nodules and carbonate concretions in the Upper Devonian shale succession of western New York-a record of variable methane flux during burial[J]. Marine and Petroleum Geology, 2015, 59: 305-319.

115 Hendry J P, Pearson M J, Trewin N H, et al. Jurassic septarian concretions from NW Scotland record interdependent bacterial, physical and chemical processes of marine mudrock diagenesis[J]. Sedimentology, 2006, 53(3): 537-565.

116 Torres M E, McManus J, Huh C A. Fluid seepage along the San Clemente Fault scarp: basin-wide impact on barium cycling[J]. Earth and Planetary Science Letters, 2002, 203(1): 181-194.

117 Aquilina L, Dia A N, Boulégue J, et al. Massive barite deposits in the convergent margin off Peru: implications for fluid circulation within subduction zones[J]. Geochimica et Cosmochimica Acta, 1997, 61(6): 1233-1245.

118 Suess E, Bohrmann G, von Huene R, et al. Fluid venting in the eastern Aleutian subduction zone[J]. Journal of Geophysical Research, 1998, 103(B2): 2597-2614.

119 Fu Baoshan, Aharon P, Byerly G, et al. Barite chimneys on the Gulf of Mexico slope: Initial report on their petrography and geochemistry [J]. Geo-Marine Letters, 1994, 14(2): 81-87.

120 Torres M E, Bohrmann G, Suess E. Authigenic barites and fluxes of barium associated with fluid seeps in the Peru subduction zone[J]. Earth and Planetary Science Letters, 1996, 144(3/4): 469-481.

121 Shields G A, Deynoux M, Strauss H, et al. Barite-bearing cap dolostones of the Taoudéni Basin, northwest Africa: Sedimentary and isotopic evidence for methane seepage after a Neoproterozoic glaciation [J]. Precambrian Research, 2007, 153(3/4): 209-235.

122 McQuay E L, Torres M E, Collier R W, et al. Contribution of cold seep barite to the barium geochemical budget of a marginal basin[J]. Deep Sea Research Part I: Oceanographic Research Papers, 2008, 55(6): 801-811.

123 冯东,陈多福. 海底沉积物孔隙水钡循环对天然气渗漏的指示[J]. 地球科学进展,2007,22(1):49-57. [Feng Dong, Chen Duofu. Barium cycling in pore water of seafloor sediment: Indicator of methane fluxes[J]. Advances in Earth Science, 2007, 22(1): 49-57.]

124 Bhatnagar G, Chapman W G, Dickens G R, et al. Sulfate-methane transition as a proxy for average methane hydrate saturation in marine sediments[J]. Geophysical Research Letters, 2008, 35(3): L03611.

125 Shields G A. A normalised seawater strontium isotope curve: possible implications for Neoproterozoic-Cambrian weathering rates and the further oxygenation of the Earth[J]. Earth, 2007, 2(2): 35-42.

126 Canet C, Anadón P, González-Partida E, et al. Paleozoic bedded barite deposits from Sonora (NW Mexico): evidence for a hydrocarbon seep environment of formation[J]. Ore Geology Reviews, 2014, 56: 292-300.

127 Guo Qingjun, Shields G A, Liu Congqiang, et al. Trace element chemostratigraphy of two Ediacaran – Cambrian successions in South China: implications for organosedimentary metal enrichment and silicification in the Early Cambrian[J]. Palaeogeography, Palaeocli-

matology, Palaeoecology, 2007, 254(1/2): 194-216.

128 Wang Jianguo, Chen Daizhao, Wang Dan, et al. Petrology and geochemistry of chert on the marginal zone of Yangtze Platform, western Hunan, South China, during the Ediacaran – Cambrian transition [J]. Sedimentology, 2012, 59(3): 809-829.

129 Wang Zhongcheng, Li Guizhi. Barite and witherite deposits in Lower Cambrian shales of South China: stratigraphic distribution and geochemical characterization[J]. Economic Geology, 1991, 86(2): 354-363.

130 杨瑞东,魏怀瑞,鲍淼,等. 贵州天柱上公塘—大河边寒武纪重晶石矿床海底热水喷流沉积结构、构造特征[J]. 地质论评,2007,53(5):675-680. [Yang Ruidong, Wei Huairui, Bao Miao, et al. Submarine hydrothermal venting—Flowing sedimentary characters of the Cambrian Shanggongtang and Dahebian barite deposits, Tianzhu county, Guizhou province[J]. Geological Review, 2007, 53(5): 675-680.]

131 刘家军,吴胜华,柳振江,等. 南秦岭大型钡成矿带中毒重石矿床成因新认识——来自单个流体包裹体证据[J]. 地学前缘,2010,17(2):222-238. [Liu Jiajun, Wu Shenghua, Liu Zhenjiang, et al. A discussion on the origin of witherite deposits in large-scale barium metallogenic belt, southern Qinling Mountains, China: evidence from individual fluid inclusion[J]. Earth Science Frontiers, 2010, 17(2): 222-238.]

132 Xu Lingang, Lehmann B, Mao Jingwen, et al. Strontium, sulfur, carbon, and oxygen isotope geochemistry of the Early Cambrian strata-bound barite and witherite deposits of the Qinling-Daba Region, Northern Margin of the Yangtze Craton, China[J]. Economic Geology, 2016, 111(3): 695-718.

133 Elswick E R, Maynard J B. Bedded barite deposits: environments of deposition, styles of mineralization, and tectonic settings[M]//Holland H D, Turekian K K, Holland H D. Treatise on Geochemistry. 2nd ed. Amsterdam: Elsevier, 2014: 629-656.

134 Pi Daohui, Jiang Shaoyong, Luo Li, et al. Depositional environments for stratiform witherite deposits in the Lower Cambrian black shale sequence of the Yangtze Platform, southern Qinling region, SW China: evidence from redox-sensitive trace element geochemistry [J]. Palaeogeography, Palaeoclimatology, Palaeoecology, 2014, 398: 125-131.

135 Han Shanchu, Hu Kai, Cao Jian, et al. Origin of early Cambrian black-shale-hosted barite deposits in South China: mineralogical and geochemical studies [J]. Journal of Asian Earth Sciences, 2015, 106: 79-94.

136 孙泽航,胡凯,韩善楚,等. 湘黔新晃—天柱重晶石矿床微量稀土元素和硫同位素研究[J]. 高校地质学报,2015,21(4):701-710. [Sun Zehang, Hu Kai, Han Shanchu, et al. Trace and rare earth elements and sulfur isotope analysis of barite deposits in West Hunan and East Guizhou [J]. Geological Journal of China Universities, 2015, 21(4): 701-710.]

137 吴朝东,陈其英,雷家锦. 湘西震旦—寒武纪黑色岩系的有机岩石学特征及其形成条件[J]. 岩石学报,1999,15(3):453-462. [Wu Chaodong, Chen Qiying, Lei Jiajin. The genesis factors and organic petrology of black shale series from the Upper Sinian to the Lower Cambrian, southwest of China[J]. Acta Petrologica Sinica, 1999, 15(3): 453-462.]

138 刘家军,吴胜华,柳振江,等. 扬子地块北缘大型钡成矿带中硫同位素组成及其意义[J]. 矿物岩石地球化学通报,2008,27(3):269-275. [Liu Jiajun, Wu Shenghua, Liu Zhenjiang, et al. Sulfur isotopic compositions of the large barium metallogenic belt in the northern Yangtze Block and its significance[J]. Bulletin of Mineralogy, Petrology and Geochemistry, 2008, 27(3): 269-275.]

139 杨瑞东,鲍淼,魏怀瑞,等. 贵州天柱寒武系底部重晶石矿床中热水生物群的发现及意义[J]. 自然科学进展,2007,17(9):1304-1309. [Yang Ruidong, Bao Miao, Wei Huairui, et al. Discovery of hydrothermal venting community at the base of Cambrian barite in Guizhou province, western China: implication for the Cambrian biological explosion[J]. Progress in Natural Science, 2007, 17(9): 1304-1309.]

140 王忠诚,储雪蕾,李仲. 高 $\delta^{34}S$ 值重晶石矿床的成因解释[J]. 地质科学,1993,28(2):191-192. [Wang Zhongcheng, Chu Xuelei, Li Zhong. Original explanation on the high $\delta^{34}S$ values of a barite deposit[J]. Scientia Geologica Sinica, 1993, 28(2): 191-192.]

141 吴胜华,刘家军,张鼐,等. 南秦岭钡成矿带重晶石与毒重石成矿特征[J]. 现代地质,2010,24(2):237-244. [Wu Shenghua, Liu Jiajun, Zhang Nai, et al. Metallogenic characteristics of barite and witherite of the Barium Metallogenic Belt in Southern Qinling Mountains[J]. Geoscience, 2010, 24(2): 237-244.]

142 吴朝东,杨承运,陈其英. 新晃贡溪—天柱大河边重晶石矿床热水沉积成因探讨[J]. 北京大学学报:自然科学版,1999,35(6):774-785. [Wu Chaodong, Yang Chengyun, Chen Qiying. The hydrothermal sedimentary genesis of barite deposits in west Hunan and East Guizhou[J]. Acta Scientiarum Naturalium Universitatis Pekinensis, 1999, 35(6): 774-785.]

143 吴卫芳,潘家永,夏菲,等. 贵州天柱大河边重晶石矿床硫同位素研究[J]. 东华理工大学学报:自然科学版,2009,32(3):205-208. [Wu Weifang, Pan Jiayong, Xia Fei, et al. Sulfur isotope of the Dahebian barite deposit, Tianzhu, Guizhou province[J]. Journal of East China Institute of Technology, 2009, 32(3): 205-208.]

144 Goldberg T, Poulton S W, Strauss H. Sulphur and oxygen isotope signatures of late Neoproterozoic to early Cambrian sulphate, Yangtze Platform, China: diagenetic constraints and seawater evolution[J]. Precambrian Research, 2005, 137(3/4): 223-241.

145 夏菲,马东升,潘家永,等. 贵州天柱大河边和玉屏重晶石矿床热水沉积成因的锶同位素证据[J]. 科学通报,2004,49(24):2592-2595. [Xia Fei, Ma Dongsheng, Pan Jiayong, et al. Strontium isotopic signature of hydrothermal sedimentation from Early Cambrian barite deposits in east Guizhou, China[J]. Chinese Science Bulletin, 2004, 49(24): 2592-2595.]

146 王忠诚,储雪蕾. 早寒武世重晶石与毒重石的锶同位素比值[J]. 科学通报,1993,38(16):1490-1492. [Wang Zhongcheng, Chu Xuelei. Strontium isotopic composition of the Early Cambrian Barite and witherite deposits[J]. Chinese Science Bulletin, 1993, 38(16): 1490-1492.]

147 Maloof A C, Porter S M, Moore J L, et al. The earliest Cambrian record of animals and ocean geochemical change[J]. Geological Society of America Bulletin, 2010, 122(11/12): 1731-1774.

148 吕志成,刘丛强,刘家军,等. 南秦岭毒重石成矿带矿床中的生物成因重晶石及其意义[J]. 自然科学进展,2004,14(8):892-897. [Lü Zhicheng, Liu Congqiang, Liu Jiajun, et al. Biogentic barite in the large barium metallogenic belt, southern Qingling Mountains and its significance[J]. Progress in Natural Science, 2004, 14(8): 892-897.]

149 吴朝东. 湘西震旦—寒武纪交替时期古海洋环境的恢复[J]. 地学前缘,2000,7(增刊Ⅰ):45-57. [Wu Chaodong. Recovery of the paleoocean environment in the alternating epoch of Late Sinian and Early Cambrian in the west Hu´nan[J]. Earth Science Frontiers, 2000, 7(Suppl. Ⅰ): 45-57.]

150 Chen Daizhao, Wang Jianguo, Qing Hairuo, et al. Hydrothermal venting activities in the Early Cambrian, South China: petrological, geochronological and stable isotopic constraints[J]. Chemical Geology, 2009, 258(3/4): 168-181.

151 Emsbo P, Hofstra A H, Johnson C A, et al. Lower Cambrian metallogenesis of south China: interplay between diverse basinal hydrothermal fluids and marine chemistry[M]//Mao Jingwen, Bierlein F P. Mineral Deposit Research: Meeting the Global Challenge: Proceedings of the 8th Biennial SGA Meeting. Berlin Heidelberg: Springer, 2005: 115-118.

152 方维萱,胡瑞忠,苏文超,等. 大河边—新晃超大型重晶石矿床地球化学特征及形成的地质背景[J]. 岩石学报,2002,18(2):247-256. [Fang Weixuan, Hu Ruizhong, Su Wenchao, et al. Geochemical characteristics of Dahebian-Gongxi Superlarge barite deposits and analysis on its background of tectonic geology, China[J]. Acta Petrologica Sinica, 2002, 18(2): 247-256.]

153 韩善楚,胡凯,曹剑. 华南早寒武世黑色岩系重晶石矿床环带钡冰长石新发现及其意义[J]. 地质论评,2013,59(6):1143-1149. [Han Shanchu, Hu Kai, Cao Jian. First discovery of zoned hyalophane in the barite deposits hosted in early cambrian black shales of south china and its geological implications[J]. Geological Review, 2013, 59(6): 1143-1149.]

154 夏菲,马东升,潘家永,等. 天柱大河边—新晃重晶石矿床矿物组成特征的电子探针研究[J]. 矿物学报,2005,25(3):289-294. [Xia Fei, Ma Dongsheng, Pan Jiayong, et al. EMP study of Early Cambrian barite deposits in eastern Guizhou, China[J]. Acta Mineralogica Sinica, 2005, 25(3): 289-294.]

155 Butterfield N J. Animals and the invention of the Phanerozoic Earth system[J]. Trends in Ecology & Evolution, 2011, 26(2): 81-87.

156 Butterfield N J. Oxygen, animals and oceanic ventilation: an alternative view[J]. Geobiology, 2009, 7(1): 1-7.

157 Canfield D E, Farquhar J. Animal evolution, bioturbation, and the sulfate concentration of the oceans[J]. Proceedings of the National Academy of Sciences of the United States of America, 2009, 106(20): 8123-8127.

Genetic Classification of Sedimentary Barites and Discussion on the Origin of the Lower Cambrian Barite-rich Deposits in the Yangtze Block, South China

ZHOU XiQiang[1] YU Hao[2] HUANG TaiYu[1,3] ZHANG LiYu[1,3]
ZHANG GongJing[1,3] FU Yong[4] CHEN DaiZhao[1]

(1. **Key Lab of Petroleum Resources Research**, **Institute of Geology and Geophysics**, **Chinese Academy of Sciences**, **Beijing** 100029, **China**;
2. **China Minmetals Corporation**, **Beijing** 100007, **China**; 3. **University of Chinese Academy of Sciences**, **Beijing** 100049, **China**;
4. **College of Resource and Environmental Engineering**, **Guizhou University**, **Guiyang** 550025, **China**)

Abstract: Barites are widely distributed in sedimentary records with various geological characteristics and formation processes. In general, sedimentary barites can be subdivided into marine (or biogenic), hydrothermal, diagenetic and cold seeps barites. The sedimentary environments, macro- and micro-occurrences, geochemical features (especially Sr and S isotopes) and corresponding geological implications of these four barite subtypes are controlled by the origin of barium- and sulfate- fluids (seawater, diagenetic porewater or hydrothermal fluids) and related interaction process (in seawater column, sediment column, sediment-water interface or hydrothermal system). In addition, this study further introduces the geological features of the Lower Cambrian barite-rich sediments in the Yangtze Block, South China, and summarizes the enrichment mechanisms having been proposed for these barite deposits and argues on their reconciliation and biases with geological features and processes. Based on the paleo-oceanic context during the Ediacaran-Cambrian transitional period, integrated sedimentological and geochemical researches together would provide better constrains on the origins of the Lower Cambrian barium-rich deposits in the Yangtze Block.

Key words: Barite; Paleo-ocean; the Lower Cambrian